NDT Advance Access published October 21, 2009

Nephrol Dial Transplant (2009) 1 of 8
doi: 10.1093/ndt/gfp553

Original Article

NDT
Nephrology Dialysis Transplantation

Renal phenotype of the cystinosis mouse model is dependent upon genetic background

Nathalie Nevo[1,2,†], Marie Chol[1,2,†], Anne Bailleux[1,2], Vasiliki Kalatzis[3,4], Ludivine Morisset[1,2], Olivier Devuyst[5], Marie-Claire Gubler[1,2] and Corinne Antignac[1,2,6]

[1]Inserm, U574, Hôpital Necker-Enfants Malades, Paris, France, [2]Université Paris Descartes, Faculté de Médecine René Descartes, Paris, France, [3]Institut de Génétique Moléculaire de Montpellier, CNRS, Montpellier, France, [4]Universités Montpellier I et II, Montpellier, France, [5]Division of Nephrology, Université Catholique de Louvain, Brussels, Belgium and [6]Assistance Publique-Hôpitaux de Paris, Service de Génétique, Hôpital Necker-Enfants Malades, Paris, France

Correspondence and offprint requests to: Corinne Antignac; E-mail: corinne.antignac@inserm.fr
[†]Nathalie Nevo and Marie Chol contributed equally to this work

Abstract

Background. Cystinosis is caused by mutations in *CTNS* that encodes cystinosin, the lysosomal cystine transporter. The most severe and frequent form is characterized by a proximal tubulopathy that appears around 6 to 12 months of age. In the absence of treatment, end-stage renal disease is reached by 10 years. $Ctns^{-/-}$ mice of a mixed 129Sv × C57BL/6 genetic background show elevated renal cystine levels; however, proximal tubulopathy or end-stage renal disease is not observed.

Methods. As renal phenotype can be influenced by genetic background, we generated congenic C57BL/6 and FVB/N $Ctns^{-/-}$ mice and assayed renal lesions and function by histological and biochemical studies.

Results. C57BL/6 $Ctns^{-/-}$ mice showed significantly higher renal cystine levels than the FVB/N strain. Moreover, C57BL/6 mice presented with pronounced histological lesions of the proximal tubules as well as a tubulopathy and progressively developed chronic renal failure. In contrast, renal dysfunction was not observed in the FVB/N strain.

Conclusions. Thus, the C57BL/6 strain represents the first $Ctns^{-/-}$ mouse model to show clear renal defects. In addition to highlighting the influence of genetic background on phenotype, the C57BL/6 $Ctns^{-/-}$ mice represent a useful model for further understanding cystinosin function in the kidney and, specifically, in the proximal tubules.

Keywords: chronic renal failure; cystinosis; genetic background; mouse model; proximal tubule dysfunction

Introduction

Cystinosis is an inherited disorder caused by mutations in the *CTNS* gene, which encodes cystinosin, the lysosomal cystine transporter [1]. Defective or absent cystinosin prevents cystine efflux thus resulting in lysosomal cystine storage [2]. At high concentrations, free cystine becomes insoluble and eventually forms crystals in certain tissues [3].

Individuals affected with the severe infantile form (MIM 219800) of the disease develop a proximal tubulopathy (de Toni-Debré-Fanconi syndrome) by 6 to 12 months of age. In the absence of treatment, end-stage renal disease (ESRD) can occur by 10 years. Also within the first year of life, cystine crystals begin to appear in the cornea, which lead progressively to severe photophobia. Continuous widespread cystine storage results in a multisystemic disorder mainly comprising growth retardation, diabetes, portal hypertension, hypogonadism, hypothyroidism, progressive muscle atrophy and weakness and central nervous system deterioration [4]. Treatment with cysteamine depletes lysosomal cystine content and postpones the deterioration of renal function and the occurrence of extra-renal organ damage; however, it is ineffective against the proximal tubulopathy [5,6].

Juvenile (MIM 219900) and ocular (MIM 219750) cystinosis are two allelic but less severe forms of the disease [7]. Juvenile cystinosis appears between 12 and 15 years and is characterized by photophobia and a glomerulopathy that slowly progresses to ESRD but not necessarily by a proximal tubulopathy [4]. The ocular form of cystinosis solely consists of corneal crystal deposits leading to mild photophobia [8].

We previously generated a mixed 129Sv × C57BL/6 strain of *Ctns*-null ($Ctns^{-/-}$) mice [9]. $Ctns^{-/-}$ mice showed cystine storage from birth in different organs (liver, kidney, lung, spleen, muscle and brain) and developed ocular changes similar to those of patients, bone defects and behavioural anomalies. Interestingly, despite elevated renal cystine levels, the proximal tubules in general did not show histological lesions, and renal dysfunction did not develop up to 18 months of age.

As renal phenotype can be dependent upon genetic background, we generated congenic C57BL/6 and FVB/N *Ctns*$^{-/-}$ mouse strains with the aim of obtaining a mouse model displaying a cystinosis-associated nephropathy. Here, we describe the first *Ctns*$^{-/-}$ mouse model to show clear renal defects: C57BL/6 *Ctns*$^{-/-}$ mice accumulated cystine and developed histological renal lesions associated with a tubulopathy. Renal dysfunction appeared by 10 months of age. By contrast, no renal alterations were observed in the FVB/N *Ctns*$^{-/-}$ mice confirming the influence of genetic background.

Materials and methods

Generation of congenic Ctns$^{-/-}$ strains

Ctns$^{-/-}$ mice were originally generated on a mixed 129Sv × C57BL/6 genetic background by replacing the last four exons of *Ctns*, which encode the last five transmembrane domains of cystinosin, with an IRES-*βgal-neo* cassette [9]. In humans, mutations in these domains lead to the same infantile cystinosis phenotype that results from complete *CTNS* deletion [10]. Consistently, the truncated murine cystinosin does not transport cystine *in vitro* [9]. Mixed-strain *Ctns*$^{+/-}$ mice were then backcrossed with wild-type C57BL/6 and FVB/N mice for 10 generations at the Centre de Distribution, Typage et Archivage animal (Centre National de la Recherche Scientifique, Orléans, France) to generate congenic mice. The offspring were genotyped to select for *Ctns* heterozygotes as previously described [9]. Thereafter, congenic *Ctns*$^{+/-}$ mice were mated to obtain C57BL/6 and FVB/N *Ctns*$^{+/+}$ and *Ctns*$^{-/-}$ mice. Weight, fertility and transmission of the inactivated gene were evaluated. All experiments and measurements were performed in accordance with national guidelines for the care and use of research animals.

Cystine assay

Dissected tissues were homogenized in 650 µg/ml *N*-ethylmaleide/PBS. Proteins were precipitated with 3% sulfosalicylic acid, resuspended in 0.1 M NaOH and protein concentration determined by the Lowry method [11]. Cystine content of the deproteinized supernatant was assayed by radiocompetition with ^{14}C-cystine (Perkin-Elmer Life Sciences, Villebon-sur-Yvette, France) for the cystine-binding protein (Riverside Scientific Enterprises, Bainbridge Island, WA, USA) as previously described [12].

Plasma and urine analysis

Blood was collected from the ocular sinus of anaesthetized mice. Urine was collected over 24 h in metabolic cages, and diuresis was measured. Plasma creatinine levels were measured by high-pressure liquid chromatography (HPLC) using a Dionex-500 system consisting of an AS50 autosampler, a GP50 gradient pump and an AD20 UV absorbance detector 220 nm. Urinary creatinine levels and urinary and plasma levels of urea, protein, glucose and electrolytes were assayed using an Olympus AU-400 multiparametric analyzer or a Beckman Synchron CX5 analyzer. Urinary pH was measured using a SP28X pH electrode and a Mettler Toledo DL 50 titrator. Urine levels of CC16 (Clara cell protein of 16 kDa), a marker of low molecular weight proteinuria indicative of proximal tubule dysfunction, were determined by immunoassay [13–15]; amino acid levels were determined by ion exchange chromatography in an AminoTac amino acid analyser, and osmolarity was determined using a Roebling automatic osmometer.

Histological studies

Kidneys were fixed for 2 h in alcoholic Bouin and transferred to 4% neutral-buffered formalin for 12 to 24 h prior to paraffin embedding. Sections were stained with either periodic acid Schiff and haematoxylin or Sirius red. For immunohistochemistry studies, all sections were pre-incubated with 3% hydrogen peroxide and blocked in 10% FCS/PBS. Slides were incubated for 1 h at room temperature (RT) with a biotinylated *Lotus tetragonolobus* lectin (LT lectin) antibody (Vector Laboratories, Burlingame, CA, USA; 1:50 dilution) or overnight at 4°C with an anti-human Tamm–Horsfall glycoprotein antibody (AbD Serotec, Cergy Saint-Christophe, France; 1:200 dilution) and then incubated for 1 h at RT with biotinylated rabbit anti-goat immunoglobulins (DAKO, Glostrup, Denmark; 1:500 di-

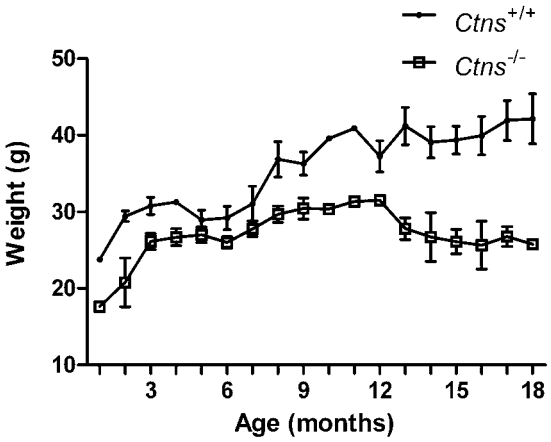

Fig. 1. Weight of congenic C57BL/6 *Ctns*$^{+/+}$ *and Ctns*$^{-/-}$ mice. C57BL/6 *Ctns*$^{+/+}$ (n = 13) and *Ctns*$^{-/-}$ (n = 11) mice were weighed periodically from 1 to 18 months of age.

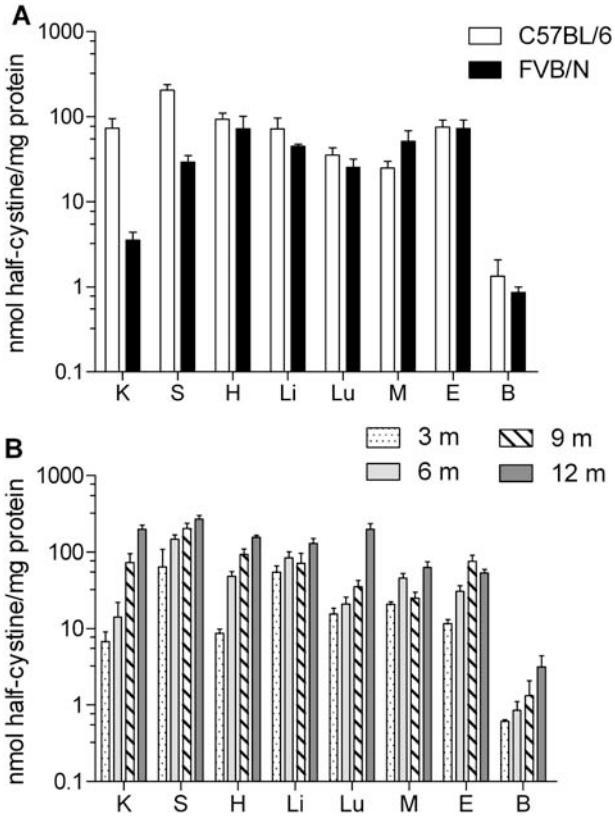

Fig. 2. Cystine levels in congenic C57BL/6 and FVB/N *Ctns*$^{-/-}$ mice. (**A**) Relative cystine levels in different tissues of 9-month-old C57BL/6 (n = 4) and FVB/N (n = 4) *Ctns*$^{-/-}$ mice. (**B**) Evolution of cystine levels in different tissues in 3-, 6-, 9- and 12-month-old C57BL/6 *Ctns*$^{-/-}$ mice (n = 4 for each group). K = kidney, S = spleen, H = heart, Li = liver, Lu = lung, M = muscle, E = eye and B = brain.

Table 1. Urine and plasma values in 2- to 18-month-old C57BL/6 *Ctns*$^{+/+}$ and *Ctns*$^{-/-}$ mice

	Ctns$^{+/+}$ 2 to 9 months	*Ctns*$^{-/-}$ 2 to 9 months	*Ctns*$^{+/+}$ 10 to 18 months	*Ctns*$^{-/-}$ 10 to 18 months
Urine values				
Number of samples	17	22	10	12
Diuresis (ml/24 h)	0.56 ± 0.06	0.92 ± 0.06***	0.84 ± 0.10	2.34 ± 0.32***
Osmolarity (mosmol/l)	1821 ± 308.5	1445 ± 56.57	1792 ± 200.5	842.2 ± 47.44***
Creatinine (mmol/l)	4.80 ± 0.44	4.83 ± 0.32	6.18 ± 0.82	2.15 ± 0.18***
Urea (mmol/l)	873.6 ± 83.77	773.7 ± 42.42	1051 ± 108.7	410.3 ± 19.87***
CC16 (µg/l)[a]	15.52 ± 3.12	85.03 ± 9.56****	8.25 ± 0.68	483.1 ± 183.2**
Protein (mg/24 h)	2.48 ± 0.83	3.94 ± 0.88	3.67 ± 1.26	2.58 ± 0.64
Glucose (µmol/24 h)	1.02 ± 0.12	2.84 ± 0.66***	1.25 ± 0.15	1.6 ± 0.6
Phosphate (µmol/24 h)	36.26 ± 5.05	63.9 ± 3.87***	44.18 ± 3.52	77.52 ± 7.21**
Sodium (µmol/24 h)	39.16 ± 5.01	55.27 ± 6.65	48.09 ± 9.47	79.88 ± 14.22
Potassium (µmol/24 h)	99.45 ± 11.86	154.3 ± 11.69**	159.6 ± 17.97	231.2 ± 25.4*
Chloride (µmol/24 h)	36.43 ± 4.87	44.06 ± 8.19	63.45 ± 18.82	87.36 ± 22.28
Plasma				
Number of samples	4	9	4	5
Creatinine (µmol/l)	7.79 ± 0.29	7.26 ± 0.46	6.96 ± 1.08	17.13 ± 2.68*
Number of samples	12	20	8	11
Urea (mmol/l)	8.65 ± 0.61	8.37 ± 0.42	9.44 ± 0.76	15.99 ± 1.77**
Proteins (g/l)	50.7 ± 0.81	51.11 ± 0.63	51.66 ± 1.47	47.93 ± 4.25
Glucose (mmol/l)	10.87 ± 0.56	11.02 ± 0.37	8.79 ± 0.27	8.43 ± 0.46
Phosphate (mmol/l)	1.99 ± 0.13	2.01 ± 0.11	1.59 ± 0.16	2.09 ± 0.16*
Sodium (mmol/l)	160.2 ± 3.06	159.6 ± 1.31	158.3 ± 2.12	158.8 ± 1.44
Potassium (mmol/l)	5.27 ± 0.28	4.77 ± 0.16Z	4.47 ± 0.37	5.65 ± 0.34*
Chloride (mmol/l)	115.3 ± 1.59	114.4 ± 0.35	112.9 ± 1.14	116 ± 1
Calcium (mmol/l)	2.05 ± 0.03	2.05 ± 0.02	2.05 ± 0.03	2.09 ± 0.04
Clearance				
Number of samples	4	9	6	5
Creatinine (ml/min)	0.37 ± 0.08	0.42 ± 0.05	0.53 ± 0.10	0.21 ± 0.05*

*$P < 0.05$; **$P < 0.01$; ***$P < 0.005$; ****$P < 0.0001$ *vs*. age-matched *Ctns*$^{+/+}$ group. [a]$n = 34$ for each genotype of the 2- to 9-month-old mice and $n = 7$ for each genotype of the 10- to 18-month-old mice.

lution). Finally, slides were incubated with streptavidin–horseradish peroxidase complex reagent and counterstained with haemalun.

Transmission electron microscopy

Avertine-anaesthetized mice received an intra-cardiac perfusion of PBS and then 2.5% glutaraldehyde/PBS. Kidneys were removed, and 1 mm^3 cortical fragments were incubated in fresh 2.5% glutaraldehyde for 2 h at RT. After rinsing in PBS, samples were post-fixed in 1% buffered osmium tetroxide for 1 h, rinsed, dehydrated in graded ethanols and transferred to propylene oxide prior to embedding in epoxy resin (Epon 812, Fluka, Saint Louis, MO). Ultra-thin (85 nm) sections from selected proximal tubule areas were collected on nickel or copper grids, stained with uranyl acetate and lead citrate and observed under a Jeol JEM-100CX II transmission electron microscope.

Statistical analysis

Mendelian transmission of the mutant *Ctns* allele was evaluated using a chi-square test. Cystine accumulation and biochemical data were compared between *Ctns*$^{+/+}$ and *Ctns*$^{-/-}$ mice of each background using the Mann–Whitney *U*-test or an unpaired two-sided s Student's *t*-test as appropriate. A P value ≤0.05 was considered significant. Results are expressed as the mean ± standard error of the mean (SEM).

Results

C57BL/6 Ctns$^{-/-}$ *mice fail to thrive*

We generated 247 C57BL/6 offspring comprising 30.4% *Ctns*$^{+/+}$, 49.4% *Ctns*$^{+/-}$ and 20.2% *Ctns*$^{-/-}$, which was consistent with a Mendelian segregation ($P < 0.05$). Similarly, the 259 FVB/N offspring showed a Mendelian segregation with 27.8% *Ctns*$^{+/+}$, 45.2% *Ctns*$^{+/-}$ and 27% *Ctns*$^{-/-}$ ($P < 0.05$). Both strains of *Ctns*$^{-/-}$ mice presented normal fertility and survival rate up to 18 months of age. Interestingly, whereas the weight of FVB/N *Ctns*$^{-/-}$ mice and their wild-type littermates was similar (data not shown), the weight of C57BL/6 *Ctns*$^{-/-}$ was lower from 1 month of age, and this difference increased with age compared with wild-type littermates (Figure 1).

C57BL/6 and FVB/N Ctns$^{-/-}$ *mice accumulate cystine*

We assayed the cystine levels in kidney, spleen, heart, liver, lung, muscle, eye and brain of C57BL/6 and FVB/N *Ctns*$^{-/-}$ mice and their wild-type littermates aged 3, 6, 9, 12 and 18 months ($n = 4$ per group). Wild-type C57BL/6 and FVB/N mice did not accumulate cystine at any age (C57BL/6 *Ctns*$^{+/+}$: 0.19 ± 0.01 nmol half-cystine/mg protein, FVB/N *Ctns*$^{+/+}$: 0.29 ± 0.03 nmol half-cystine/mg protein; average values of all organs). In contrast, congenic C57BL/6 and FVB/N *Ctns*$^{-/-}$ mice showed elevated cystine levels in all tissues tested (Figure 2). However, the renal cystine levels of FVB/N *Ctns*$^{-/-}$ mice were significantly lower than those of C57BL/6 mice: 3.54 ± 0.84 nmol half-cystine/mg protein for FVB/N and 73.28 ± 21.5 nmol half-cystine/mg protein for C57Bl/6 ($P < 0.05$) *Ctns*$^{-/-}$ mice aged 9 months (Figure 2A). In both strains, the amount of stored cystine increased with age (Figure 2B for C57BL/6 mice; data not shown for FVB/N), but the renal cystine levels

Table 2. Urine and plasma values in 10- and 12-month-old C57BL/6 *Ctns*$^{+/+}$ and *Ctns*$^{-/-}$ mice

	Ctns$^{+/+}$ 10 months	*Ctns*$^{-/-}$ 10 months	*Ctns*$^{+/+}$ 12 months	*Ctns*$^{-/-}$ 12 months
Number of samples	5	5	6	6
Urine values				
Body weight (BW) (g)	30.7 ± 2.1	25.9 ± 0.7*	35.0 ± 3.4	27.0 ± 1.3***
Diuresis (µl/min/g BW)	0.05 ± 0.005	0.14 ± 0.030*	0.03 ± 0.003	0.16 ± 0.015***
pH	6.57 ± 0.20	6.49 ± 0.15	6.50 ± 0.29	6.10 ± 0.26***
Bicarbonate (mM/mM creat)	0.54 ± 0.50	1.24 ± 1.20	0.20 ± 0.14	0.19 ± 0.11
Plasma				
Creatinine (µmol/l)	8.5 ± 0.9	14.7 ± 0.6**	8.8 ± 0.9	29.2 ± 3.5***
Urea (mmol/l)	8.5 ± 0.7	11.8 ± 1.0*	11.5 ± 0.8	22.5 ± 2.0***
Bicarbonate (mmol/l)	17.3 ± 1.2	15.8 ± 1.6	13.9 ± 0.8	14.2 ± 0.6
Sodium (mmol/l)	151 ± 0.2	151 ± 1.0	144 ± 0.4	146 ± 0.6**
Potassium (mmol/l)	4.9 ± 0.2	5.7 ± 0.8	4.0 ± 0.2	3.6 ± 0.1
Chloride (mmol/l)	113 ± 0.6	115 ± 1.0	114 ± 0.2	115 ± 0.8

*$P < 0.05$; **$P < 0.01$; ***$P < 0.005$ *vs*. age-matched *Ctns*$^{+/+}$ group.

Table 3. Daily urinary excretion of amino acids of C57BL/6 *Ctns*$^{+/+}$ and *Ctns*$^{-/-}$ mice

	Ctns$^{+/+}$ 2 to 9 months	*Ctns*$^{-/-}$ 2 to 9 months	*Ctns*$^{+/+}$ 10 to 18 months	*Ctns*$^{-/-}$ 10 to 18 months
Number of samples	17	7	20	13
(nmol/24 h)				
Aspartate	41.24 ± 8.31	58.45 ± 15.23	47.28 ± 21.67	109.5 ± 40.94
Threonine	74.82 ± 6.31	103.0 ± 10.58	95.49 ± 12.86	109.2 ± 24.09
Serine	36.02 ± 3.81	61.18 ± 8.35*	39.68 ± 6.27	69.37 ± 30.06
Asparagine	32.75 ± 3.66	61.82 ± 24.0	50.42 ± 10.17	41.2 ± 7.86
Glutamate	66.65 ± 17.04	123.9 ± 38.91	60.91 ± 23.82	146.5 ± 114.4
Glutamine	188.70 ± 19.48	242 ± 21.10	232.7 ± 33.50	210.4 ± 17.80
Proline	23.56 ± 6.88	50.45 ± 12.68	45.29 ± 0	118.9 ± 86.39
Glycine	293.20 ± 35.88	355.7 ± 38.49	333.7 ± 42.01	314.1 ± 91.55
Alanine	103.20 ± 14.34	165.2 ± 25.15*	148.5 ± 24.27	160.2 ± 68.40
Citrulline	33.44 ± 4.07	40.0 ± 5.55	33.58 ± 6.35	40.35 ± 9.0
Valine	59.56 ± 6.42	76.0 ± 12.25	71.67 ± 14.12	87.06 ± 25.83
½ cystine	78.53 ± 22.97	222.9 ± 77.25	32.63 ± 8.07	125.5 ± 17.64**
Methionine	16.54 ± 3.12	27.47 ± 5.72	19.49 ± 3.25	78.06 ± 46.51
Isoleucine	16.78 ± 1.93	27.06 ± 6.32	20.98 ± 3.68	40.37 ± 20.56
Leucine	40.28 ± 7.99	57.75 ± 11.13	37.94 ± 5.49	59.11 ± 35.66
Tyrosine	151.80 ± 23.49	195 ± 22.5	167.3 ± 39.15	259.3 ± 64.95
Phenylalanine	20.71 ± 2.74	33.15 ± 23.75	24.98 ± 8.09	42.41 ± 30.33
Ornithine	23.93 ± 2.63	29.33 ± 3.83	23.02 ± 4.18	32.62 ± 4.91
Lysine	130.2 ± 17.1	146.3 ± 19.70	173.9 ± 57.23	229.2 ± 62.78
Histidine	51.91 ± 11.58	65.76 ± 13.80	0 ± 0	49.3 ± 10.80
Arginine	26.30 ± 3.47	24.81 ± 3.41	21.74 ± 5.31	53.47 ± 25.88

*$P < 0.05$; **$P < 0.01$ *vs*. age-matched *Ctns*$^{+/+}$ group.

were consistently lower in FVB/N *Ctns*$^{-/-}$ mice. Thus, at 18 months of age, the renal levels of FVB/N (29.27 ± 6.28 nmol half-cystine/mg protein, $n = 8$) were considerably lower than those of younger (12-month-old) C57BL/6 (198.9 ± 25.8 nmol half-cystine/mg protein) *Ctns*$^{-/-}$ mice.

C57BL/6 Ctns$^{-/-}$*mice develop proximal tubule dysfunction and progressive chronic renal failure*

We screened C57BL/6 *Ctns*$^{-/-}$ mice for tubular dysfunction. Polyuria was detected from 2 months and worsened with age and was linked to a concentration defect as shown by progressive decrease in urinary osmolarity (Table 1). An increased daily excretion of glucose, phosphate, and potassium was observed in 2- to 9-month-old animals. In addition, we observed a marked increase in CC16 excretion in 2- to 9-month-old mice, indicative of low molecular weight proteinuria and confirming the presence of early proximal tubular dysfunction (Table 1). Furthermore, we analysed acid–base parameters in two additional independent cohorts of C57BL/6 mice. Ten-month-old *Ctns*$^{-/-}$ mice with mild renal failure had plasma bicarbonate levels and urine pH values similar to control mice. Urinary excretion levels of bicarbonate were highly variable but not significantly different from those of *Ctns*$^{+/+}$ mice. In contrast, 12-month-old *Ctns*$^{-/-}$ mice were characterized by renal failure and lower urine pH as compared with wild-type littermates. The urinary excretion of bicarbonate was highly variable but not significantly different from controls (Table 2). Urinary amino acid levels were not modi-

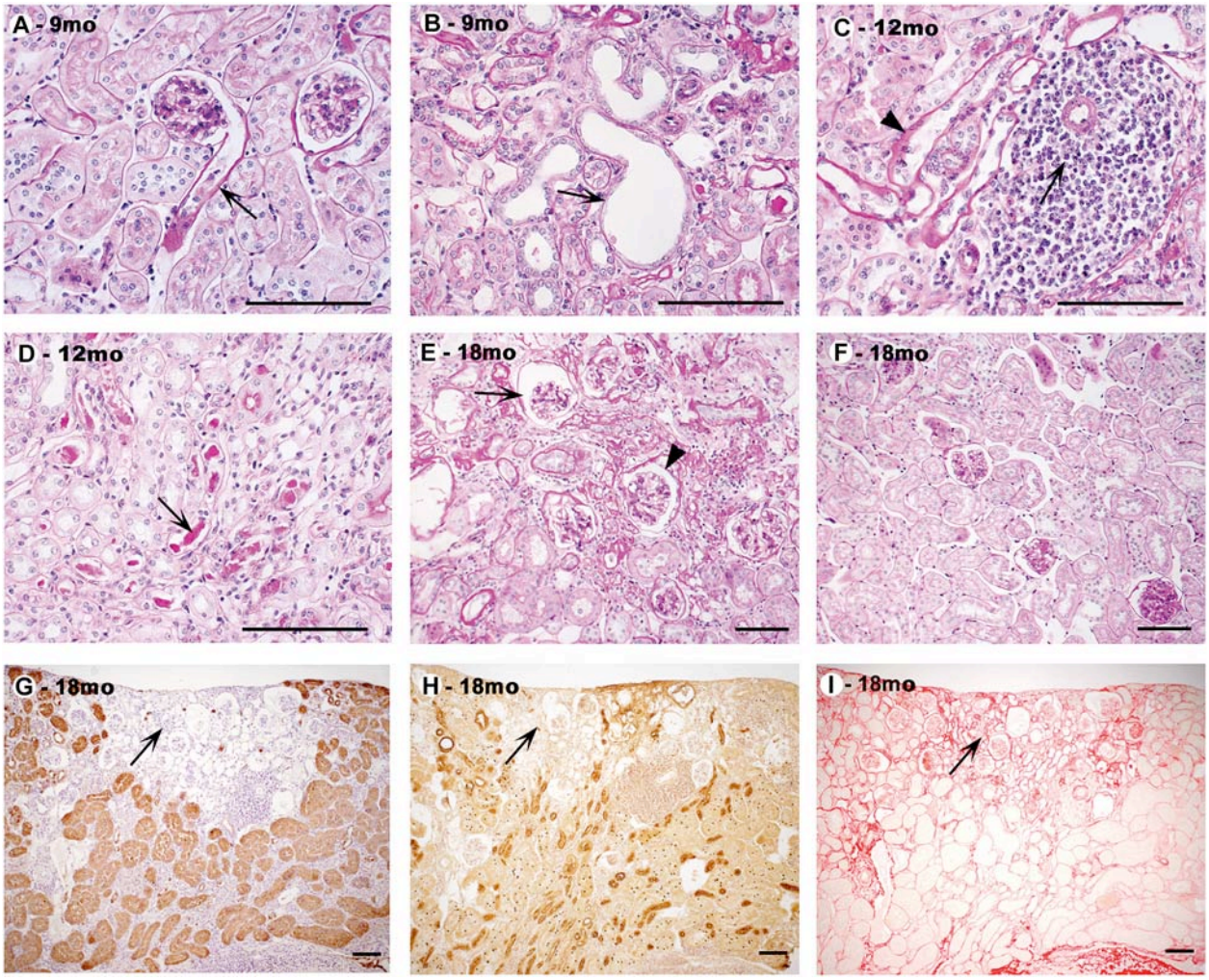

Fig. 3. Histological lesions in C57BL/6 *Ctns*$^{-/-}$ mice. Staining with periodic acid Schiff and hematoxylin (**A–F**). (A) Proximal tubular atrophy and thickening of the basement membrane (arrow), (B) tubular dilatation and epithelial layer effacement (arrow), (C) cellular infiltration (arrow), tubular atrophy and thickening of basement membrane (arrowhead), (D) tubular cast (arrow). Magnification ×40. (E) Collapsed (arrow) and sclerosed (arrowhead) glomeruli with severe tubulo-interstitial lesions, (F) wild-type C57BL/6. Magnification ×20. Serial kidney sections **(G–I)**. (G) Focal disappearance of proximal tubules (arrow; LT lectin labelling), (H) partial disappearance of TAL and DCT (arrow; Tamm–Horsfall labelling), (I) thickened basement membrane and mild interstitial fibrosis (arrow; Sirius red staining). Magnification ×10. The age of the corresponding mouse is indicated on each photo. Scale bar represents 100 μm.

fied except for a 4-fold increase in cystine levels in older mice (Table 3). This increase could be explained by renal cell peeling off and thus could not be considered as a consequence of the proximal tubulopathy. Up to 9 months, no plasma abnormalities were detected. Subsequently, 10- to 18-month-old *Ctns*$^{-/-}$ mice developed chronic renal failure as indicated by progressive diminution of creatinine clearance (Table 1).

We did not detect any evident anomalies in FVB/N *Ctns*$^{-/-}$ mice up to 18 months of age (data not shown).

C57BL/6 Ctns$^{-/-}$ *mice progressively develop pronounced renal lesions*

Kidneys from C57BL/6 and FVB/N wild-type and *Ctns*$^{-/-}$ mice were screened at 3, 6, 9, 12 and 18 months for renal lesions. In C57BL/6 *Ctns*$^{-/-}$ mice, we did not detect lesions at 3 months. In contrast at 6 months, the mice developed focal lesions affecting proximal tubules, mostly in the superficial cortex. They were more extensive at 9 months, but their severity and extent varied from case to case. The lesions were characterized by atrophy to complete disappearance of the epithelial cell layer associated with thickening of the basement membrane, evident in the initial part of the tubule (Figure 3A), or dilatation of the tubular lumen lined by dedifferentiated epithelial cells (Figure 3B). In addition, tubular casts were focally present in the medullary tubules (data not shown). At 12 months, tubular atrophy was more extensive and focally associated with inflammatory infiltrates (Figure 3C) and tubular casts at the corticomedullary junction (Figure 3D). At 18 months, multiple and large cortical foci of severely atrophic tubules were observed. In these areas, proximal tubules were not recognizable; the glomerular tufts were preserved or collapsed, and/or sclerotic, mild interstitial fibrosis and focal infiltration were associated (Figure 3E).

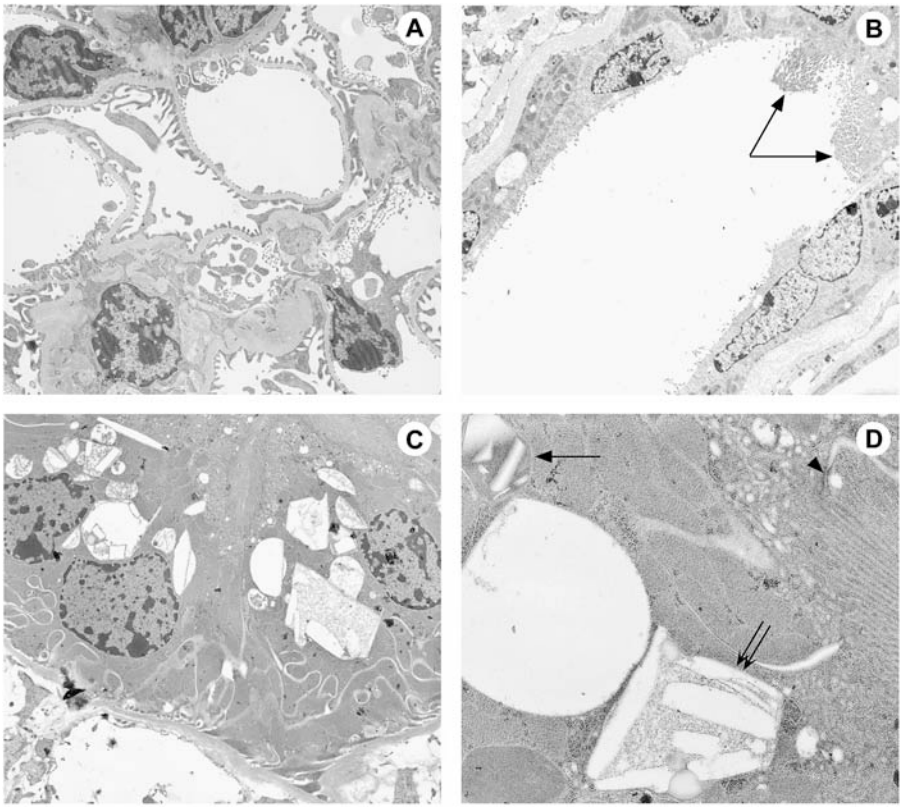

Fig. 4. Electron microscopy of the kidney cortex of a 10-month-old C57BL/6 *Ctns*$^{-/-}$ mouse. (**A**) Glomerulus with normal differentiation of podocyte foot processes. No cystine crytals can be seen. Magnification ×2700. (**B**) Severe proximal tubular atrophy with persistence of a dystrophic brush border (arrows). Magnification ×2000. (**C**) Extensive lysosomal accumulation of cystine crystals of various sizes and forms in two adjacent well-differentiated proximal tubular cells. Magnification ×2700. (**D**) High magnification of part of a proximal tubular cell with cystine crystals (arrow) and an autophagic vacuole (double arrow). Note the preservation of the brush border, the tight junction (arrowhead) and the vacuolar apparatus. Magnification ×10 000.

Interestingly, between focal scars, the parenchyma was normal. In the medulla, tubules were totally collapsed or filled with protein casts, giving the appearance of thyroid-like structures. Vessels were normal throughout the kidneys (data not shown). We did not detect any of the aforementioned alterations on kidney sections of wild-type C57BL/6 mice aged 3 to 18 months (Figure 3F).

In order to better characterize the renal lesions in C57BL/6 *Ctns*$^{-/-}$ mice, we stained serial kidney sections with proximal tubule (LT lectin) or thick ascending loop of Henle (TAL) and distal convoluted tubule (DCT) (Tamm–Horsfall protein) markers. In 9- and 12-month-old mice, disappearance or faint and irregular LT lectin staining of atrophic tubules was observed, whereas the expression of the Tamm–Horsfall protein was normal, confirming that proximal lesions occur first (data not shown). At 18 months, in the most severely affected areas, proximal tubules had almost completely disappeared as demonstrated by the absence of LT lectin labelling (Figure 3G). When still present, they were vacuolated and atrophic. Progressively, TALs and DCTs were also affected (Figure 3H). Mild fibrosis was associated (Figure 3I). The absence of fibrosis in 9- and 12-month-old mice with focal tubular lesions suggests that tubular damage precedes fibrosis. Normal expression of the different markers was observed in wild-type mice aged 3 to 18 months (data not shown).

We also studied the aspect of the kidneys of *Ctns*$^{-/-}$ mice aged 9 to 11 months by transmission electron microscopy. Glomeruli were normal or showed focal non-specific retraction and sclerosis of the tuft (Figure 4A). Proximal tubule alterations were highly irregular and consisted mostly of dedifferentiation: collapsed or dilated tubules were surrounded by a thick basement membrane and were lined by flat cells that showed complete loss or focal persistence of the brush border (Figure 4B). In a few proximal tubular cells with preserved differentiation (brush border and vacuolar apparatus), cystine crystals of varying sizes were observed (Figure 4C and D). Strikingly, numerous tubules of normal appearance were adjacent to injured tubules.

Lastly, no renal lesions were detected in FVB/N *Ctns*$^{-/-}$ animals up to 18 months of age (data not shown). Taken together, our results show that C57BL/6 *Ctns*$^{-/-}$ mice develop histological renal lesions mainly characterized by focal tubular atrophy, which appear by 6 months and involve primarily the proximal tubules. Following tubular atrophy, interstitial fibrosis develops, and the lesions extend. At 18 months, most of the cortex is affected.

Discussion

Patients with the infantile cystinosis develop a severe nephropathy early in childhood, characterized by a proximal

tubulopathy that eventually leads to end-stage renal disease before 10 years of age in the absence of treatment [4,16]. We previously generated *Ctns*$^{-/-}$ mice on a mixed 129Sv × C57BL/6 background. Although *Ctns*$^{-/-}$ mice developed bone and ocular abnormalities as seen in patients, we did not detect an obvious renal phenotype despite elevated cystine levels [9].

Mouse models of other renal pathologies have also been generated on mixed genetic backgrounds, and the results have been variable regarding the reproduction of the disease. The animal models of s Dent's disease, a nephrolithiasis disorder [15], or MODY3 diabetes [17,18] resulted in a renal phenotype similar to that seen in patients. In contrast, the mouse model of Gitelman syndrome (lacking the Na–Cl$^-$ co-transporter NCCT) generated on a mixed genetic background did not present essential features of the disease [19]. However, when these mice were backcrossed to generate a congenic C57BL/6 mouse model, the renal phenotype was faithfully reproduced [20,21].

Therefore, in an effort to obtain a *Ctns*$^{-/-}$ mouse model displaying a cystinosis-associated nephropathy and to assess the possible role of genetic background, we generated two congenic C57BL/6 and FVB/N *Ctns*$^{-/-}$ mouse strains. Both strains showed normal fertility and survival rate, but the C57BL/6 *Ctns*$^{-/-}$ mice presented with growth retardation from birth that worsened with age. Moreover, *Ctns*$^{-/-}$ mice of both strains accumulated cystine in different tissues, although only the C57BL/6 mice displayed a clear renal phenotype.

The discrepancy between the presence and absence of a renal phenotype in the two strains could be partially due to the lower amounts of renal cystine accumulation in FVB/N than in C57BL/6 *Ctns*$^{-/-}$ mice. Consistently, the mixed 129Sv × C57BL/6 *Ctns*$^{-/-}$ mouse strain contained half the amount of renal cystine as compared to the congenic C57BL/6 strain and also did not show renal dysfunction. The reason for the lower cystine levels in the congenic FVB/N or mixed 129Sv *Ctns*$^{-/-}$ strains is currently unknown but could be explained by the presence of an alternative pathway of cystine export from the lysosome, as has been previously hypothesized [22] and that is more efficient in FVB/N mice. Alternatively, modifier genes differentially expressed in each strain may modulate or compensate the effect of the truncated *Ctns* [23,24]. Along this line, a comparative study of the existing *Ctns*$^{-/-}$ lines may identify loci modifying the extent and progression of renal disease.

Congenic C57BL/6 *Ctns*$^{-/-}$ mice develop a tubulopathy, characterized by polyuria, increased glucose, phosphate and potassium urinary daily excretion and low molecular weight proteinuria, which progresses to chronic renal failure. The tubulopathy mimics the phenotype described in patients with cystinosis. However, aminoaciduria, bicarbonaturia and sodium loss are absent. Renal insufficiency appears from 10 months of age. Histologically, the lesions affect primarily the proximal tubules in cystinotic mice as in patients [3]. However, contrary to the diffuse changes observed in patients, the tubular lesions have a focal distribution in *Ctns*$^{-/-}$ mice. The focal origin of the lesions remains to be explained; however, it may be noteworthy that intranephron segmental heterogeneity has been documented previously in mice in terms of proximal tubular endocytic uptake [25]. Furthermore, compensatory mechanisms in a mouse model of proximal tubule dysfunction have also been shown to have a focal nature [26].

The type of proximal tubular anomaly also differs between cystinosis patients and mice. Marked heterogeneity in the shape and size of proximal tubules as well as unequal appearance of tubular cells within a tubular section are early hallmarks of infantile cystinosis [3]. By contrast, in C57Bl/6 *Ctns*$^{-/-}$ mice, the kidneys appear initially normal, then focal tubular atrophy or dedifferentiation occurs. Their initial location in the most proximal part of the tubules is, however, reminiscent of the swan-neck lesion described in patients [27]. Similarly, the nearly complete disappearance of tubular structures observed focally in *Ctns*$^{-/-}$ mice is reminiscent of the diffuse atrophy of end-stage kidneys associated with infantile cystinosis. In all cases, even in severely damaged *Ctns*$^{-/-}$ mouse kidneys, the interstitial fibrosis around atrophic tubules remained mild. The same discrepancy between the severity of tubular lesions and fibrosis was also observed in patients. The multinucleated giant podocytes frequently observed in patients were never seen in the mouse kidneys.

Thus, the congenic C57BL/6 mouse model of cystinosis develops a proximal tubulopathy associated with extensive histological lesions and chronic renal failure. These defects were not observed in FVB/N *Ctns*$^{-/-}$ mice. Given the important role played by the genetic background in this model, further analysis of the differences between the two strains should allow a better understanding of the pathophysiology of cystinosis. Although the renal phenotype of the C57BL/6 *Ctns*$^{-/-}$ mice does not completely mimic the human disease, this mouse strain is the first available cystinosis animal model to present clear renal defects. Encouragingly, we previously showed that the congenic C57BL/6 *Ctns*$^{-/-}$ mice mimic disease in terms of ocular anomalies [28]. Furthermore, we showed that progressive cystine accumulation in the central nervous system of these animals results in age-related learning and memory impairments that parallel those of cystinosis patients [29]. Thus, in addition to representing a more appropriate model for cystinosis, the congenic C57BL/6 mouse strain may contribute to understanding the mechanisms involved in renal impairment in cystinosis patients and to testing emerging therapeutics.

Acknowledgements. This work was funded by the 'Association pour l'Information et la Recherche sur les Maladies Rénales Génétiques' (Ph.D. grant to M.C.); the Cystinosis Research Foundation (Post-doctoral grant to A.B.); 'Vaincre les Maladies Lysosomales'; the Cystinosis Research Network; the Belgian Fonds National de la Recherche Scientifique and Fonds de la Recherche Scientifique Médicale; the Alphonse & Jean Forton Foundation; the Concerted Research Action (05/10-328); the Inter-university Attraction Pole (P6/05), and EUNEFRON (FP7, GA#201590). We thank Nicolas Sorhaindo (Université Paris 7, France) and Afrem Aydin (UCL, Brussels, Belgium) for biochemical analyses and Yvette Cnops (UCL) for CC16 immunoassay. We thank Dominique Eladari (UMRS872, Paris, France) for help with mouse phenotype characterization and Daniel Rabier (Hôpital Necker-Enfants Malades, Paris, France) for biochemistry studies.

Conflict of interest statement. None declared.

References

1. Town M, Jean G, Cherqui S *et al*. A novel gene encoding an integral membrane protein is mutated in nephropathic cystinosis. *Nat Genet* 1998; 18: 319–324
2. Kalatzis V, Cherqui S, Antignac C *et al*. Cystinosin, the protein defective in cystinosis, is a H()-driven lysosomal cystine transporter. *Embo J* 2001; 20: 5940–5949
3. Gubler MC, Lacoste M, Sich M *et al*. The pathology of the kidney in cystinosis. In: M Broyer (ed). *Cystinosis.* Paris: Elsevier, 1999; 42–48
4. Gahl WA, Schneider JA, Aula P. Lysosomal transport disorders: cystinosis and sialic acid storage disorders. In: CL Scriver, AL Beaudet, WS Sly, D Valle (eds). *The Metabolic and Molecular Basis of Inherited Disease.* New York: McGraw-ill, 2001; 5085–5108
5. Thoene JG, Oshima RG, Crawhall JC *et al*. Cystinosis. Intracellular cystine depletion by aminothiols in vitro and in vivo. *J Clin Invest* 1976; 58: 180–189
6. Gahl WA, Thoene JG, Schneider JA. Cystinosis. *N Engl J Med* 2002; 347: 111–121
7. Kalatzis V, Antignac C. Cystinosis: from gene to disease. *Nephrol Dial Transplant* 2002; 17: 1883–1886
8. Anikster Y, Lucero C, Guo J *et al*. Ocular nonnephropathic cystinosis: clinical, biochemical, and molecular correlations. *Pediatr Res* 2000; 47: 17–23
9. Cherqui S, Sevin C, Hamard G *et al*. Intralysosomal cystine accumulation in mice lacking cystinosin, the protein defective in cystinosis. *Mol Cell Biol* 2002; 22: 7622–7632
10. Attard M, Jean G, Forestier L *et al*. Severity of phenotype in cystinosis varies with mutations in the CTNS gene: predicted effect on the model of cystinosin. *Hum Mol Genet* 1999; 8: 2507–2514
11. Lowry OH, Rosebrough NJ, Farr AL *et al*. Protein measurement with the Folin phenol reagent. *J Biol Chem* 1951; 193: 265–275
12. Oshima RG, Willis RC, Furlong CE *et al*. Binding assays for amino acids. The utilization of a cystine binding protein from *Escherichia coli* for the determination of acid-soluble cystine in small physiological samples. *J Biol Chem* 1974; 249: 6033–6039
13. Bernard A, Lauwerys R, Noel A *et al*. Determination by latex immunoassay of protein 1 in normal and pathological urine. *Clin Chim Acta* 1991; 201: 231–245
14. Bernard AM, Thielemans NO, Lauwerys RR. Urinary protein 1 or Clara cell protein: a new sensitive marker of proximal tubular dysfunction. *Kidney Int Suppl* 1994; 47: S34–37
15. Wang SS, Devuyst O, Courtoy PJ *et al*. Mice lacking renal chloride channel, CLC-5, are a model for Dent's disease, a nephrolithiasis disorder associated with defective receptor-mediated endocytosis. *Hum Mol Genet* 2000; 9: 2937–2945
16. Niaudet P, Tête MJ, Broyer M. Renal disease in cystinosis. In: M Broyer (ed). *Cystinosis.* Paris: Elsevier, 1999; 36–41
17. Pontoglio M, Prie D, Cheret C *et al*. HNF1alpha controls renal glucose reabsorption in mouse and man. *EMBO Rep* 2000; 1: 359–365
18. Pontoglio M, Barra J, Hadchouel M *et al*. Hepatocyte nuclear factor 1 inactivation results in hepatic dysfunction, phenylketonuria, and renal Fanconi syndrome. *Cell* 1996; 84: 575–585
19. Schultheis PJ, Lorenz JN, Meneton P *et al*. Phenotype resembling Gitelman's syndrome in mice lacking the apical Na+-Cl− cotransporter of the distal convoluted tubule. *J Biol Chem* 1998; 273: 29150–29155
20. Loffing J, Vallon V, Loffing-Cueni D *et al*. Altered renal distal tubule structure and renal Na(+) and Ca(2+) handling in a mouse model for Gitelman's syndrome. *J Am Soc Nephrol* 2004; 15: 2276–2288
21. Morris RG, Hoorn EJ, Knepper MA. Hypokalemia in a mouse model of Gitelman's syndrome. *Am J Physiol Renal Physiol* 2006; 290: F1416–1420
22. Greene AA, Marcusson EG, Morell GP *et al*. Characterization of the lysosomal cystine transport system in mouse L-929 fibroblasts. *J Biol Chem* 1990; 265: 9888–9895
23. Ratelade J, Lavin TA, Muda AO *et al*. Maternal environment interacts with modifier genes to influence progression of nephrotic syndrome. *J Am Soc Nephrol* 2008; 19: 1491–1499
24. Andrews KL, Mudd JL, Li C *et al*. Quantitative trait loci influence renal disease progression in a mouse model of Alport syndrome. *Am J Pathol* 2002; 160: 721–730
25. Caplanusi A, Parreira KS, Lima WR *et al*. Intravital multi-photon microscopy reveals several levels of heterogeneity in endocytic uptake by mouse renal proximal tubules. *J Cell Mol Med* 2008; 12: 351–354
26. Gailly P, Jouret F, Martin D *et al*. A novel renal carbonic anhydrase type III plays a role in proximal tubule dysfunction. *Kidney Int* 2008; 74: 52–61
27. Mahoney CP, Striker GE. Early development of the renal lesions in infantile cystinosis. *Pediatr Nephrol* 2000; 15: 50–56
28. Kalatzis V, Serratrice N, Hippert C *et al*. The ocular anomalies in a cystinosis animal model mimic disease pathogenesis. *Pediatr Res* 2007; 62: 156–162
29. Maurice T, Hippert C, Serratrice N *et al*. Cystine accumulation in the CNS results in severe age-related memory deficits. *Neurobiol Aging* 2009; 30: 987–1000

Received for publication: 20.7.09; Accepted in revised form: 22.9.09